Chapter 2
Concepts and Methodology of Interaction of Carbon Nanostructures with Cellular Systems

Alexandre L.R. de Oliveira, Helder J. Ceragioli, and Kyl Assaf

Abstract Carbon nanostructures have been shown to have a wide range of applications in several fields. However, characterization seems to be a key factor in order to make data comparable. In this sense, the present chapter addresses important techniques and approaches to provide fundamental information regarding purification and structure of carbon nanoparticles including SEM, FESEM, TEM, Raman, FTIR, and AFM, as tools for spectroscopy and morphology of the samples. Additionally to that, functionalization of nanotubes and graphene with some chemical groups is addressed providing basis for enhancing the biological and functional properties of the nanostructures. Finally, we address different applications of carbon nanoparticles in medical and biological areas, including tumor research, cell culture peripheral nerve regeneration, stem cell therapy, and applications as biosensors.

2.1 Functionalization

2.1.1 Attachment of Oxidic Groups

One of the most common functionalization techniques is the oxidation of nanotubes by liquid phase or gas phase, introducing carboxylic groups and some other oxygen-bearing functionalities such as hydroxyl, carbonyl, ester, and nitro groups (nitro is

A.L.R. de Oliveira (✉) • K. Assaf
Department of Structural and Functional Biology, Institute of Biology, University of Campinas – UNICAMP, Campinas, São Paulo, Brazil
e-mail: alroliv@unicamp.br

H.J. Ceragioli
Faculty of Electric Engineering and Computation (FEEC), University of Campinas – UNICAMP, Campinas, São Paulo, Brazil

N. Durán et al. (eds.), *Nanotoxicology*, Nanomedicine and Nanotoxicology,
DOI 10.1007/978-1-4614-8993-1_2, © Springer Science+Business Media New York 2014

not considered an oxidic group as hydroxyl or carbonyl ones, please see this concept) into the tubes (Hirsch and Vostrowsky 2005).

The development of an oxidation process for SWCNTs (single-walled carbon nanotubes) involves extensive ultrasonic treatment in a mixture of concentrated nitric and sulfuric acid. Such drastic conditions lead to the opening of the tube caps as well as the formation of holes in the sidewalls, followed by an oxidative etching along the walls with the concomitant release of carbon dioxide. The final products are nanotube fragments with lengths in the range of 100–300 nm, whose ends and sidewalls are decorated with a high density of various oxygen-containing groups (mainly carboxyl groups). Under less vigorous conditions, such as refluxing in nitric acid, the shortening of the tubes can be minimized. The chemical modification is then limited mostly to the opening of the tube caps and the formation of functional groups at defect sites along the sidewalls. Nanotubes functionalized in this manner basically retain their pristine electronic and mechanical properties (Zhang et al. 2003; Balasubramanian and Burghard 2005).

The oxidative introduced carboxyl groups represent useful sites for further modifications as they enable the covalent coupling of molecules through the creation of amide and ester bonds. By this method the nanotubes can be provided with a wide range of functional moieties for which purpose bifunctional molecules (e.g., diamines) are often utilized as linkers. Illustrative examples are nanotubes equipped with dendrimers, nucleic acids, enzymes, metal complexes, or semiconductor and metal nanoparticles (Zhang et al. 2003; Katz and Willner 2004; Balasubramanian and Burghard 2005). Another interesting application of the carboxyl groups is the formation of an anhydride at the tube ends through which rings of nanotubes are accessible. The presence of (modified) carboxyl groups leads to a reduction of van der Waals interactions between the CNTs, which strongly facilitates the separation of nanotube bundles into individual tubes. Additionally, the attachment of suitable groups renders the tubes soluble in aqueous or organic solvents, opening the possibility of further modifications through subsequent solution-based chemistry. A high water solubility of a few tenths of a gram per milliliter has recently been achieved on the basis of the carboxyl-based coupling of hydrophilic polymers such as poly(ethylene glycol) (PEG) (Zhang et al. 2003; Fernando et al. 2004; Katz and Willner 2004; Balasubramanian and Burghard 2005). SWCNTs with a good solubility in organic solvents can be obtained by covalent (Hamon et al. 1999; Zhang et al. 2003; Fernando et al. 2004; Katz and Willner 2004; Balasubramanian and Burghard 2005) or ionic (Hamon et al. 1999; Chen et al. 2001; Zhang et al. 2003; Fernando et al. 2004; Katz and Willner 2004; Balasubramanian and Burghard 2005) attachment of long-chain aliphatic amines onto the carboxyl groups.

2.1.2 Amidation

The introduction of carboxylic groups to nanotubes by oxidative procedures gives access to a large number of functional exploitations by transformation of the carboxylic functions and provides anchor groups for further modification. From carboxylic acids, carboxamides can be formed via carboxylic acid chlorides and allow for the decoration of oxidized tubes with aliphatic amines, aryl amines, amino acid derivatives, peptides, amino-group-substituted dendrimers, etc. as nucleophiles. The carboxylic groups can be activated by conversion into acyl chloride groups with thionyl chloride (Chan et al. 2006; Chen et al. 2001), and the acyl chlorides formed can be transformed to carboxamides by amidation. Similarly, carboxamide nanotubes have been prepared using dicyclohexylcarbodiimide (DCC) as dehydrating agent and allowing the direct coupling of amines and carboxylic functions under mild, neutral conditions (Hirsch and Vostrowsky 2005).

Hamon et al. (2002) were the first to report the functionalization of oxidatively treated SWCNTs with alkyl amines and less nucleophilic aniline derivatives (Chen et al. 1988, 2001; Liu et al. 1998; Hirsch and Vostrowsky 2005; Tasis et al. 2006). The conversion of the acid functionality to the amide of octadecylamine led to the first shortened, soluble SWCNTs. The analysis of (end group and defect site) octadecylamido (ODA)-functionalized SWCNTs by solution phase mid-IR spectroscopy showed that the weight percentage of the acylamido functionality was about 50 % (Func CNT) (Chen et al. 1988, 2001; Liu et al. 1998; Marcoux et al. 2004; Hirsch and Vostrowsky 2005; Tasis et al. 2006). In the seminal work of Liu et al. (1998), it was demonstrated that the groups generated by the acid-cut nanotubes were carboxylates, which could be derivatized chemically by thiolalkylamines through amidation reaction. The resulting material could be visualized by AFM imaging after tethering gold nanoparticles to the thiol moieties. It was demonstrated that nanotube tips can be created by coupling basic or biomolecular probes to the carboxylic groups that are present at the open ends (Woolley et al. 2000). These modified nanotubes were used as AFM tips to titrate acids and bases, to image patterned samples based on molecular interactions, and to measure binding forces between single protein-ligand pairs 139c SWCNT tips. Images recorded on patterned SAMs enabled true molecular-resolution imaging (Tasis et al. 2006).

Chen et al. (2001) treated oxidized nanotubes with long-chain alkylamines via acylation and made for the first time the functionalized material soluble in organic solvents (Fig. 2.1). Further studies showed that 4-alkylanilines could also give soluble material, 140 whereas the presence of the long alkyl chain played a critical role in the solubilization process.

Esterification reactions resulted also in soluble functionalized nanotubes (Hamon et al. 2002). The photochemical behavior of soluble alkyl ester-modified nanotubes gave rise to measurable photocurrents after illuminating solutions of these tubes. By using time-resolved spectroscopy (laser flash photolysis), the

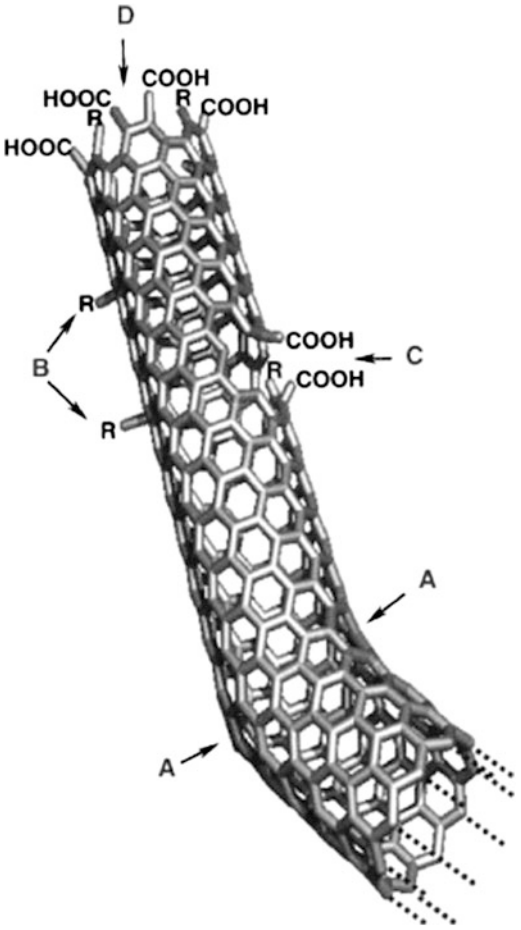


Fig. 2.1 Typical defects in a SWNT. (**a**) Five- or seven-membered rings in the carbon framework, instead of the normal six-membered ring, leads to a bend in the tube. (**b**) sp^3-hybridized defects (R═H and OH). (**c**) Carbon framework damaged by oxidative conditions, which leaves a hole lined with –COOH groups. (**d**) Open end of the SWNT, terminated with COOH groups. Besides carboxyl termini, the existence of which has been unambiguously demonstrated, other terminal groups such as $–NO_2$, –OH, –H, and = O are possible (Hirsch 2002) (www.entechopen.com)

transient spectrum of the charge separated state could be detected. Size and shape are very important issues in CNT chemistry. The change in shape from straight form to circles can have interesting implications in electronics (Liu et al. 1998; Martel et al. 1999; Woolley et al. 2000; Chen et al. 2001; Hamon et al. 2002; Marcoux et al. 2004; Tasis et al. 2006). The amidation or esterification of oxidized nanotubes has become one of the most popular ways of producing soluble materials either in organic solvents or in water.

2.1.3 Covalent Bonding

Chemical functionalization is based on the covalent bond of functional groups onto carbon form of CNTs. It can be performed at the end caps of nanotubes or at their

sidewalls which have many defects. Direct covalent sidewall functionalization is associated with a change of hybridization from sp^2 to sp^3 and a simultaneous loss of *p*-conjugation system on graphene layer (Jeon et al. 2011). This process can be made by reaction with some molecules of a high chemical reactivity. In the first approach, fluorination of CNTs has become popular for initial investigation of the covalent functionalization because the CNTs sidewalls are expected to be inert (Prato et al. 2008; Jeon et al. 2011). The fluorinated CNTs have C–F bonds that are weaker than those in alkyl fluorides (Kelly et al. 1999; Prato et al. 2008; Jeon et al. 2011) and thus providing substitution sites for additional functionalization (Kelly et al. 1999; Inahara et al. 2002; Prato et al. 2008; Jeon et al. 2011). Successful replacements of the fluorine atoms by amino, alkyl, and hydroxyl groups have been achieved. Other methods, including cycloaddition, such as Diels–Alder reaction, carbene and nitrene addition, chlorination, bromination (Kelly et al. 1999; Inahara et al. 2002; Prato et al. 2008; Jeon et al. 2011), hydrogenation, and azomethine ylides (Kelly et al. 1999; Inahara et al. 2002; Unger et al. 2002; Tagmatarchis and Prato 2004; Prato et al. 2008; Jeon et al. 2011) have also been successfully employed.

Another method is defect functionalization of CNTs. These intrinsic defects are supplemented by oxidative damage to the nanotube framework by strong acids which leave holes functionalized with oxygenated functional groups (Chen et al. 1988; Kelly et al. 1999; Inahara et al. 2002; Unger et al. 2002; Tagmatarchis and Prato 2004; Prato et al. 2008; Jeon et al. 2011). In particular, treatment of CNTs with strong acid such as HNO_3, H_2SO_4, or a mixture of them (Chen et al. 1988; Esumi et al. 1996; Kelly et al. 1999; Inahara et al. 2002; Unger et al. 2002; Tagmatarchis and Prato 2004; Prato et al. 2008; Jeon et al. 2011) or with strong oxidants such as $KMnO_4$, ozone, and reactive plasma tend to open these tubes and to subsequently generate oxygenated functional groups such as carboxylic acid, ketone, alcohol, and ester groups that serve to tether many different types of chemical moieties onto the ends and defect sites of these tubes (Jeon et al. 2011). These functional groups have rich chemistry and the CNTs can be used as precursors for further chemical reactions, such as silanation, polymer grafting, esterification, thiolation, and even some biomolecules (Jeon et al. 2011). The CNTs functionalized by the covalent methods have the major advantage of exhibiting solubility in various organic solvents because the CNTs possess many functional groups such as polar or nonpolar groups (Jeon et al. 2011). For example (Fig. 2.1), the end caps of nanotubes tend to be composed of highly curved fullerene-like hemispheres, which are therefore highly reactive as compared with the side walls (Chen et al. 1988; Esumi et al. 1996; Kelly et al. 1999; Hirsch 2002; Inahara et al. 2002; Unger et al. 2002; Tagmatarchis and Prato 2004; Prato et al. 2008; Jeon et al. 2011). The sidewalls themselves contain defect sites such as pentagon–heptagon pairs called Stone–Wales defects, *sp3*-hybridized defects, and vacancies in the nanotube lattice (Chen et al. 1988; Esumi et al. 1996; Kelly et al. 1999; Hirsch 2002; Inahara et al. 2002; Unger et al. 2002; Tagmatarchis and Prato 2004; Prato et al. 2008; Jeon et al. 2011).

For graphene or graphene oxide (GO), several chemical procedures have been developed to afford dispersible graphene; in principle they are based on the exfoliation of graphite, chemical or thermal reduction of GO, intercalative expansion of graphite, chemical vapor deposition, and epitaxial growth (Georgakilas et al. 2012). Pristine graphene has been isolated by sonication of graphite in organic solvents. The dispersion of graphene in organic solvents helps in the functionalization of graphene by several functional groups (Georgakilas et al. 2012).

The main purpose is the dispersibility of graphene in common organic solvents that is usually obtained after attachment of certain organic groups. The dispersion of graphene sheets in organic solvents is a crucial move toward the formation of nanocomposite materials with graphene. In addition, organic functional groups such as chromophores offer new properties that could be combined with the properties of graphene such as conductivity. In most cases when organic molecules are covalently attached on the graphene surface, its extended aromatic character is perturbed, enabling the control of its electronic properties. The development of a band gap through chemical doping is a powerful method for the use of graphene in nanoelectronic devices (Niyogi et al. 2010; Georgakilas et al. 2012). The organic covalent functionalization reactions of graphene include two general routes: (a) the formation of covalent bonds between free radicals or dienophiles and C═C bonds of pristine graphene and (b) the formation of covalent bonds between organic functional groups and the oxygen groups of GO. Based on the previous experimental and theoretical experience with fullerene and carbon nanotubes, the most attractive organic species for the reaction with sp^2 carbons of graphene are organic free radicals and dienophiles. Usually both are intermediate reactive components that are produced under certain conditions in the presence of graphene (Georgakilas et al. 2012).

2.2 Characterization Techniques

2.2.1 SEM

Research development of electron microscopes began in the 1920s. Under the guidance of Max Knoll, Ernst Ruska began work on the development of electron lenses at the Technical University of Berlin, Germany, in 1928. His work was fundamental for the subsequent creation of an electron microscope in that these lenses were needed to channel the electrons of the beam. The first functional transmission electron microscope was developed in the early 1930s by Ruska who constructed a two stage electron microscope with three magnetic lenses, condenser, objective, and projector (Stadtländer 2007; Haguenau et al. 2003). Early electron microscopic studies were primarily focused on the study of the optical behavior of electron beams under various conditions. Thus, no biological applications were initially envisioned. However, it soon became clear that the

superior magnifying power of an electron microscope could be applied to the study of the structure of various specimens, including those from plants, animals, microorganisms, and viruses (Stadtländer 2007; Haguenau et al. 2003). EM is considered today by many scientists as one of the most significant and useful developments for the ultrastructural investigation of specimens in the life sciences as well as in physics and material science (Haguenau et al. 2003). Because of the broad applications of the electron microscope to the fields of biology, medicine, and material science, Ruska received the prestigious Nobel Prize in Physics in 1986 for his fundamental work in electron optics and for the design of the first electron microscope (Stadtländer 2007).

The two basic types of electron microscopes are the scanning electron microscope and the transmission electron microscope.

Scanning electron microscopy (SEM) is a powerful method for the investigation of surface structures. This technique provides a large depth of field, which means, the area of the sample that can be viewed in focus at the same time is actually quite large. SEM has also the advantage that the range of magnification is relatively wide allowing the investigator to easily focus in on an area of interest on a specimen that was initially scanned at a lower magnification. Furthermore, the three-dimensional appearing images may be more appealing to the human eye than the two-dimensional images obtained with a transmission electron microscope. Therefore, an investigator may find it easier to interpret SEM images. Finally, the number of steps involved for preparing specimens for SEM investigation is lower and thus the entire process is less time consuming than the preparation of samples for investigation with a transmission electron microscope (Stadtländer 2007).

The first and basic part of the microscopes is the source of electrons. It is usually a V-shaped filament made of LaB6 or W (tungsten) that is wreathed with Wehnelt electrode (Wehnelt Cap). Due to negative potential of the electrode, the electrons are emitted from a small area of the filament (point source). A point source is important because it emits monochromatic electrons (with similar energy). The two usual types of electron guns are the conventional electron guns and the field emission guns (FEG) (Voutou and Stefanaki 2008).

When an electron beam interacts with the atoms in a sample, individual incident electron undergo two types of scattering—elastic and inelastic. In the former, only the trajectory changes and the kinetic energy and velocity remain constant. In the case of inelastic scattering, some incident electrons will actually collide with and displace electrons from their orbits (shells) around nuclei of atoms comprising the sample. This interaction places the atom in an excited (unstable) state. Specimen interaction is what makes electron microscopy possible. The interactions (inelastic) noted on the top side of the diagram are utilized when examining thick or bulk specimens (SEM) while on the bottom side are those examined in thin or foil specimens (transmission electron microscopy, TEM) (Voutou and Stefanaki 2008).

When a sample is bombarded with electrons, the strongest region of the electron energy spectrum is due to secondary electrons (Fig. 2.2). The secondary electron yield depends on many factors and is generally higher for high atomic number targets and at higher angles of incidence. Secondary electrons are produced when

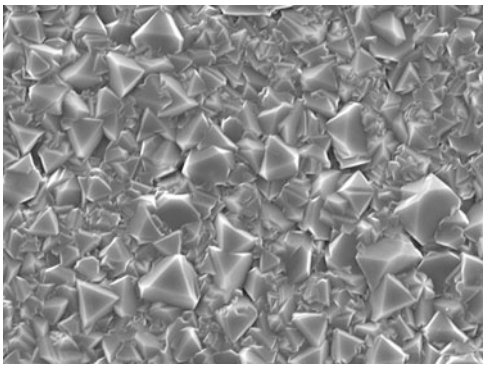


Fig. 2.2 Images of secondary electron (picture from Prof. Dr. Helder Ceragioli personal archive)

an incident electron excites an electron in the sample and loses most of its energy in the process. The excited electron moves toward the surface of the sample undergoing elastic and inelastic collisions until it reaches the surface, where it can escape if it still has sufficient energy (Voutou and Stefanaki 2008).

Backscattered electrons consist of high-energy electrons originating in the electron beam that are reflected or backscattered out of the specimen interaction volume. The production of backscattered electrons varies directly with the specimen's atomic number. This differing production rates cause higher atomic number elements to appear brighter than lower atomic number elements. This interaction is utilized to differentiate parts of the specimen that have different average atomic number (Voutou and Stefanaki 2008).

Auger electrons are electrons ejected by radiationless excitation of a target atom by the incident electron beam. When an electron from the L-shell drops to fill a vacancy formed by K-shell ionization, the resulting X-ray photon with energy EK–EL may not be emitted from the atom. If this photon strikes a lower energy electron (e.g., an M-shell electron), this outer electron may be ejected as a low energy Auger electron. Auger electrons are characteristic of the fine structure of the atom and have energies between 280 eV (carbon) and 2.1 keV (sulfur). By discriminating between Auger electrons of various energies, a chemical analysis of the specimen surface can be made. Auger electrons are exploited in Auger electron spectroscopy tools. The volume inside the specimen in which interactions occur while being struck with an electron beam is called specimen interaction volume.

2.2.2 FESEM

FESEM is the abbreviation of field emission scanning electron microscope. A FESEM is microscope that works with electrons (particles with a negative charge) instead of light. These electrons are liberated by a field emission source. The object is scanned by electrons according to a zigzag pattern. A FESEM is used to visualize very small topographic details on the surface or entire or fractioned objects.

Researchers in biology, chemistry, and physics apply this technique to observe structures that may be as small as 1 nm (= billion of a millimeter). The FESEM may be employed, for example, to study organelles and DNA material in cells, synthetical polymers, and coatings on microchips and nanomaterials (Yao and Kimura 2007).

Nanotechnology has strongly driven in the development of recent electron microscopy, with demands not only for increasing resolution but also for more information from the sample. Electron microscopes use a beam of highly energetic electrons to probe objects on a very fine scale (Pawley 1997; Wang 2000). In standard electron microscopes, electrons are mostly generated by "heating" a tungsten filament (electron gun). They are also produced by a crystal of LaB6 (define this). The use of LaB6 results in a higher electron density in the beam and a better resolution than that with the conventional device. In a field emission (FE) electron microscope, on the other hand, no heating but a so-called "cold" source is employed. Field emission is the emission of electrons from the surface of a conductor caused by a strong electric field. An extremely thin and sharp tungsten needle (tip diameter 10–100 nm) works as a cathode. The FE source reasonably combines with scanning electron microscopes (SEMs) whose development has been supported by advances in secondary electron detector technology. The acceleration voltage between cathode and anode is commonly in the order of magnitude of 0.5–30 kV, and the apparatus requires an extreme vacuum (~10^{-6} Pa) in the column of the microscope. Because the electron beam produced by the FE source is about 1,000 times smaller than that in a standard microscope with a thermal electron gun, the image quality will be markedly improved; for example, resolution is on the order of ~2 nm at 1 keV and ~1 nm at 15 keV. Therefore, the FESEM is a very useful tool for high-resolution surface imaging in the fields of nanomaterials science (Yao and Kimura 2007).

The electron beam is focused by the electromagnetic lenses (condenser lens, scan coils, stigmator coils, and objective lens) and the apertures in the column to a tiny sharp spot.

The image is formed when the primary probe bombards the object and secondary electrons are emitted from the object surface with a certain velocity that is determined by the levels and angles at the surface of the object. The secondary electrons, which are attracted by the Corona, strike the scintillator (fluorescing mirror) that produces photons. The location and intensity of illumination of the mirror vary depending on the properties of the secondary electrons. The signal produced by the scintillator is amplified and transduced to a video signal that is fed to a cathode ray tube in synchrony with the scan movement of the electron beam. The contrast in the "real time" image that appears on the screen reflects the structure on the surface of the object. Parallel to the analog image, a digital image is generated which can be further processed (Fig. 2.3).

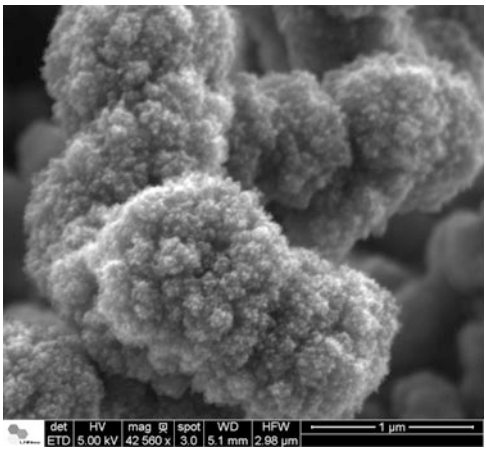


Fig. 2.3 FESEM image of carbon nanoparticle (picture from Prof. Dr. Helder Ceragioli personal archive)

2.2.3 TEM

Transmission electron microscopy (TEM) is a technique where an electron beam interacts and passes through a specimen. The electrons are emitted by a source and are focused and magnified by a system of magnetic lenses. The electron beam is confined by the two condenser lenses which also control the brightness of the beam, passes the condenser aperture, and "hits" the sample surface. The electrons that are elastically scattered consist the transmitted beams, which pass through the objective lens. The objective lens forms the image display and the following apertures, the objective and selected area aperture are used to choose of the elastically scattered electrons that will form the image of the microscope. Finally, the beam goes to the magnifying system that is consisted of three lenses, the first and second intermediate lenses which control the magnification of the image and the projector lens. The formed image is shown either on a fluorescent screen or in monitor or both and is printed on a photographic film (Voutou and Stefanaki 2008).

The operation of TEM requires an ultrahigh vacuum and a high voltage. The first step is to find the electron beam, so the lights of the room must be turned off. Through a sequence of buttons and adjustments of focus and brightness of the beam, we can adjust the settings of the microscope so that by shifting the sample holder find the thin area of the sample. Then, tilting of the sample begins by rotating the holder (Voutou and Stefanaki 2008). This is a way to observe as much areas as we can, so we can obtain as much information as well. Different types of images are obtained in TEM using the apertures properly and the different types of electrons. As a result, diffraction patterns are shown because of the scattered electrons. If the unscattered beam is selected, we obtain the bright field image. Dark field images are attained if diffracted beams are selected by the objective aperture. Also in TEM, analysis is done with EDX (energy dispersive X-ray), EELS (electron energy loss spectrum), and EFTEM (energy-filtered transmission electron microscopy).

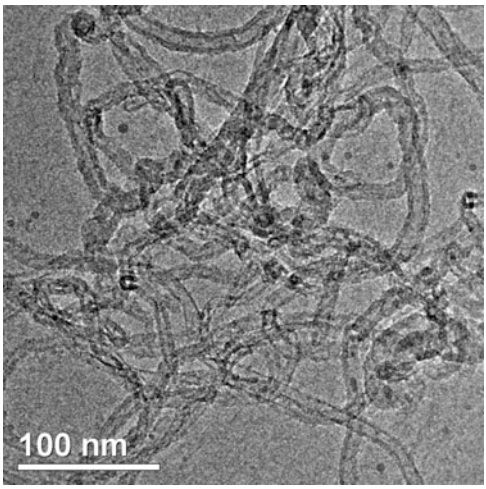


Fig. 2.4 Transmission electron microscopy image (picture from Prof. Dr. Helder Ceragioli personal archive)

In transmission microscopy, we can actually see the specimen's structure and its atomic columns; thus, compositional and crystallographic information is attained. However, expertise is needed and the sample preparation phase is too difficult so that very thin samples are achieved. The first step is to decide whether the sample is useful to be observed and in which view, plan or cross section. Due to the strong interaction between electrons and matter, the specimens have to be rather thin, less than 100 nm. This is achieved with several methods, depending on the material. The sample preparation is a precise and a severe procedure, which may affects the results of the microscopic analysis and study.

Transmission microscopy provides several types of images (Fig. 2.4) as reported above. The diffraction patterns show dots, regions, or circles originating from the sample area illuminated by the electron beam that depends on the material's structure. Monocrystals show distinguished dots in diffraction patterns, polycrystalline materials' common centered circles, and amorphous materials' diffused circles. Distortions and defects are visible in bright and dark field images, but expertise is needed in order to interpret whether they are defects or artifacts. Electron or ion beam damages must be considered in TEM analysis because of the sensibility of the sample and its really low thickness.

Additionally, there is always the problem of calibration and alignment of the instrument. Both of them require experience and skills, so the resulting images and data that emerge are reliable and free of objective astigmatism. These works have to be done in order to keep the instrument in excellent working condition. TEM provides accurate measurements and studies in different types of materials, given that observations are in atomic scale in HRTEM (define this). Transmission electron microscopes offer resolutions up to 0.1 nm at 300 kV and probe diameters up to 0.34 nm (Voutou and Stefanaki 2008).

2.2.4 Raman

Chandrasekhara Venkata Raman discovered the Raman effect; he began his scientific research into the scattering of light, the work that led to his discovery of the Raman effect in 1928, for which he was awarded the Nobel Prize in record time, just 2 years later.

The technique consists in an inelastic process that occurs when a sample is illuminated with a monochromatic light source, such as a laser beam. In this process, energy from the incident photons is transferred to the sample molecules, exciting them to high vibrational modes. Scattered photons have a lower frequency than the incident ones due to the energy transfer (Guimarães et al. 2006; Moreira et al. 2008).

The irradiation of a molecule with a monochromatic light always results in two types of light scattering, elastic and inelastic. In elastic scattering, there occurs no change in photon frequency or without any change in its wavelength and energy. Conversely, the other is inelastic scattering which is accompanied by the shift in photon frequency due to excitation or deactivation of molecular vibrations in which either the photon may lose some amount of energy or gains energy (Das and Agrawal 2011). Thus, three types of phenomena can occur (Das and Agrawal 2011; Fig. 2.5).

First, when light is incident on a molecule, it can interact with the molecule but the net exchange of energy (E) is zero, so the frequency of the scattered light is the same as that of the incident light ($E = E_o$). This process is known as Rayleigh scattering (Das and Agrawal 2011).

Second, the light can interact with the molecule and the net exchange of energy is the energy of one molecular vibration. If the interaction causes the light photon to gain vibrational energy from the molecule, then the frequency of the scattered light will be higher than that of the incident light, known as anti-Stokes Raman scattering (Das and Agrawal 2011).

Third, if the interaction causes the molecule to gain energy from the photon, then the frequency of the scattered light will be lower than that of the incident light ($E = E_o - E_v$); this process is known as Stokes Raman scattering. A Raman spectrometer is composed of light source, monochromator, sample holder and detector. The factors which affect the analysis on Raman spectra may include high signal-to-noise ratio, instrument stability, and sufficient resolution. The development of effective FT Raman spectrometers using NIR or red excitation lasers solved the problem of avoiding fluorescence that affects the Raman signals. On the other hand, the development of highly sensitive detectors in conjunction with coupling of optical fibers and microscopes enhanced the capacity of analysis (Parker 1994; Das and Agrawal 2011). Two major technologies are used to collect the Raman spectra, dispersive Raman spectroscopy and Fourier transform Raman spectroscopy, with difference in their laser sources and the way by which Raman scattering is detected and analyzed. Both these techniques have unique advantages

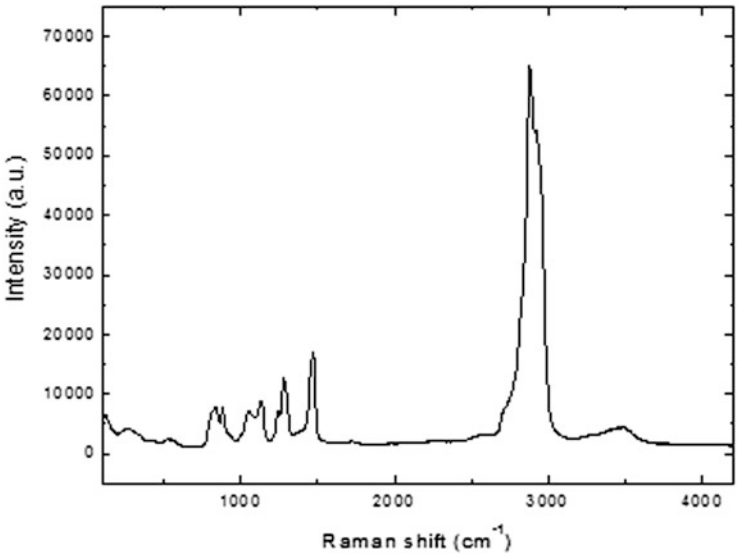


Fig. 2.5 Raman spectroscopy of poly(ethylene glycol) (picture from Prof. Dr. Helder Ceragioli personal archive)

and the method that best suit the sample should be preferred (Wang and McCreery 1989; Parker 1994; Das and Agrawal 2011).

Several type of lasers can be used as the excitation source, like argon ion (488.0 and 514.5 nm), krypton ion (530.9 and 647.1 nm), He:Ne (632.8 nm), Nd:YAG (1,064 and 532 nm), and diode laser (630 and 780 nm). Use of 1,064 nm near-IR (NIR) excitation laser causes lower fluorescent effect than visible wavelength lasers (Hanlon et al. 2000).

The Raman-scattered light can be collected by a spectrometer and displayed as a spectrum, in which its intensity is displayed as a function of its frequency change. Since each molecular species has its own unique set of molecular vibrations, the Raman spectrum of a particular species will consist of a series of peaks or bands, each shifted by one of the characteristic vibrational frequencies of that molecule. The spectrum is a plot of the scattered light intensity versus its change in frequency relative to that of the incident light (Hanlon et al. 2000). Raman frequency shifts are conventionally measured in wave numbers (cm^{-1}), a convenient unit for relating the change in vibrational energy of the scattering molecule to the change in frequency of the scattered light. 1 cm^{-1} equals 30,000 MHz; this is typically 10,000 times smaller than the frequency of the light itself. Each band of scattered light in Raman spectrum is characteristic of molecular vibrational motions, which, taken all together, are unique for PEG (Fig. 2.6). In other words, the molecular structure and composition of a material under study is encoded as a set of frequency shifts in the Raman-scattered light. Thus, the Raman spectrum can provide a

fingerprint of a substance from which the molecular composition can be determined (Hanlon et al. 2000).

Although Raman spectroscopy had been widely used for chemical and molecular analysis for many years, its application to biomedical problems is relatively recent. Raman studies of biological tissue have been facilitated over the past 10 years by advancing technology, particularly in the areas of lasers and detectors. However, the real success of these studies at providing insight into the molecular basis of disease and showing the potential for medical diagnostic applications has relied on advanced methods of analyzing tissue Raman spectra. Raman spectroscopy is a nondestructive technique with a wide range of possible applications in the field of biomedical research (Hanlon et al. 2000).

2.2.5 FTIR

FTIR spectrometers have almost entirely replaced dispersive instruments because of their improved performance in nearly all respects. The application of this technique has improved the acquisition of IR spectra dramatically. The heart of the optical hardware in such FT spectrometers is the interferometer. The classic two-beam Michelson interferometer is shown schematically in and consists of two mutually perpendicular plane mirrors: a fixed mirror and a movable one. A semi-reflecting mirror, the *beam splitter*, bisects the planes of these two mirrors. A beam emitted by a source is split in two by the beam splitter (Bunaciu et al. 2010). The reflected part of the beam travels to the fixed mirror, is reflected there, and hits the beam splitter again. The same happens to the transmitted radiation. Because the two split beams are spatially coherent, they interfere on recombination. The beam, modulated by the movement of the mirror, leaves the interferometer and is finally focused on the detector. The signal actually registered by the detector, the interferogram, is, thus, the radiation intensity of the combined beams as a function of the position of the movable mirror. The mathematics of the conversion of an interferogram into a spectrum is the Fourier transformation. Based on fully developed software, a computer performs this transformation. The essential steps for obtaining an FTIR spectrum are to produce an interferogram with and without a sample in the beam and then to transform these interferograms into spectra of the source with sample absorption and the source without sample absorption (Bunaciu et al. 2010). The ratio of the former to the latter is the IR transmission spectrum of the sample. In the case of FTIR spectroscopy, the sample is usually placed between the interferometer and the detector. In transmission measurement, the source illuminates the sample, and the detector is placed behind the sample to acquire the fraction of light transmitted through the sample. Transmission analysis requires the sample to be partly transparent. In most cases, in the MIR range, samples must be diluted in nonabsorbing (or nonabsorbent?) matrix; otherwise, no light might be transmitted to the detector. Liquid can be prepared as a dilute solution in a cell. Solid samples are dispersed usually in a potassium bromide (KBr) disk or mull (Bunaciu

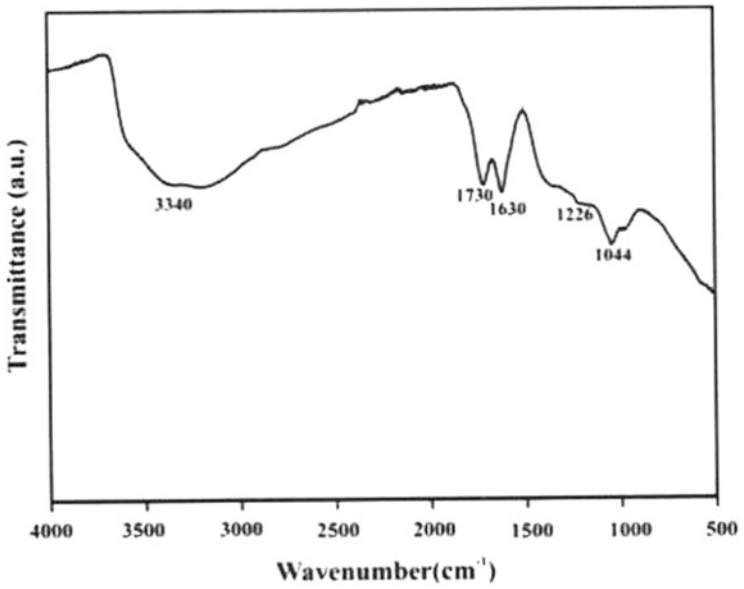


Fig. 2.6 FTIR spectrum of graphene oxide nanosheets (picture from Prof. Dr. Helder Ceragioli personal archive)

et al. 2010). Moreover, the powder particle size must be smaller than the radiation wavelength to avoid the Christiansen scattering effect, which appears as band distortion in the spectra (Bowie et al. 2002). Transmission has been extensively used to analyze thin samples such as films (Chan et al. 2006) or tissues (Krafft et al. 2006). It is not possible with thick samples such as tablets (Bunaciu et al. 2010). FTIR spectroscopy is a vibrational spectroscopic technique that can be used to optically probe the molecular changes associated with diseased tissues. The method is employed to find more conservative ways of analysis to measure characteristics within tumor tissue and cells that would allow accurate and precise assignment of the functional groups, bonding types, and molecular conformations. Spectral bands in vibrational spectra are molecule specific and provide direct information about the biochemical composition. FTIR peaks are relatively narrow and in many cases can be associated with the vibration of a particular chemical bond (or a single functional group) in the molecule (Bunaciu et al. 2010).

The characteristic FTIR spectrum of GO nanosheets (Rattanaa et al. 2012) is depicted in Fig. 2.6. It is seen with oxygen-containing groups in which the main absorption band at 3,340 cm^{-1} is assigned to the O–H group stretching vibrations. The absorption peak at 1,730 and 1,630 cm^{-1} can be assigned to C═O stretching of carboxylic and/or carbonyl moiety functional groups. The two absorption peaks at about 1,226 cm^{-1} and 1,044 cm^{-1} are assigned to the C–O stretching vibrations.

Although Raman spectroscopy and FTIR are relevant techniques, with their respective spectra complementary to one another, there are some differences

between these two techniques. Probably the most important difference is the type of samples that can be investigated by each of these methods. FTIR mainly deals with nonaqueous samples, while Raman is as effective with aqueous samples as it is with nonaqueous ones (Movasaghi et al. 2008). This is because of the problem mostly taken place with FTIR spectroscopy; the problem is due to strong absorption bands of water. In Raman, however, fluorescence and the strong effect of glass (mostly as containers) are the most significant problems during analysis. Raman requires minimal sample preparation and can perform confocal imaging, whereas FTIR requires comparatively more sample preparation and does not have the ability of confocal imaging. Furthermore, the physical effect of infrared is created by absorption and mainly influences the dipole and ionic bands such as O–H, N–H, and C═O. Raman effect originates from scattering (emission of scattered light) and changing of the polarizability of covalent bands like C═C, C–S, S–S, and aromatics. In other words, FTIR spectroscopy is due to changes in dipole moment during molecular vibration, whereas Raman spectroscopy involves a change in polarizability (Movasaghi et al. 2008).

2.2.6 AFM

The atomic force microscope (AFM) was discovered by Binnig, Quate, and Gerber (Binnig et al. 1986) and has become an important tool for imaging surfaces. The principle of AFM is based on laser tracking the deflection of microscopic-sized probe (i.e., cantilever) through its nanometer tip interacting with sample surface. The system consists of the AFM probe with a sharp nanometer-size tip mounted on each soft cantilever with specific spring constant, the piezo-control (feedback loop) system that allows for monitoring the interaction forces between the tip and sample surface and controls the piezo scanner movements through digital/analog converter, the piezoelectric scanner that moves the tip on the surface of the sample in the *x*–*y*–*z* planes, segmented photodiode detector for measuring deflections of cantilever through laser, and analog/digital converter system for recording data. AFM probes consist of a microscopic-sized rectangular or/and "V"-shaped cantilevers, typically constructed from silicon or silicon nitride, with a sharp pyramidal tip (nanometer) or glass/polystyrene beads (micrometer). The property of the soft cantilever determines the sensitivity. The dimension of the tip determines the spatial resolution of the instrument, smaller in tip size and better resolution. The tips are typically made from Si_3N_4, or Si (Wu et al. 2012).

The AFM imaging can be obtained through contact and tapping (intermittent) mode. The cantilever in AFM probe is oscillated at its resonant frequency under an external electrical excitation, lightly "taps" on the sample surface, and contacting the surface at the bottom (*z*-axis) of each swing at each given *x*–*y* point. By maintaining constant oscillation amplitude, a constant tip–sample interaction is maintained and an image of the surface is obtained (Pereira 2001). The advantages of tapping mode are that it allows high-resolution scanning of samples that are prone to be easily

damaged and could be used for freshly isolated cells that loosely held to a dish bottom. The disadvantages of tapping mode are that it does not offer a good image in liquids and slower scan speeds are needed for tapping mode operation (Wu et al. 2012).

2.3 Applications in Medical and Biological Areas

2.3.1 Tumor

The use of nanobiotechnology to reduce growth and to deliver substances directly to tumor cells is one of the most promising approaches to achieve highly efficient treatments against cancer. In this sense, nanoparticle drug delivery has been actively investigated in the recent years. The interaction between CNT with proteins and nucleic acids indicates that they may become adsorbed to the nanotube surface. Depending on the size of the molecules, they may be loaded to the interior cavity of open nanotubes as well.

Since the intracellular delivery of drugs is very complicated, CNTs may be used as carrier due to their capacity of penetrating the plasma membrane. As shown by Pantarotto et al. (2004a), functionalized carbon nanotubes accumulate in the cytoplasm and reach the nucleus in a nontoxic way up to a concentration of 10 μm. This was achieved by combining modified SWNTs with FITC (Fluorescein isothiocyanate). The process of cell penetration seems to be fast, reaching saturation points at 60 min.

The same authors have also provided data regarding plasmid DNA gene delivery (Pantarotto et al. 2004b) by the use of ammonium-functionalized CNTs. In this sense, CNTs were covalently modified and functionalized with a pyrrolidine ring. By doing this, the authors have obtained more soluble carbon nanotubes, particularly in aqueous solutions. The intracellular delivery was demonstrated in HeLa cells, observed by transmission electron microscopy. Multiwalled carbon nanotubes (MWCNT) were observed crossing the cell membrane as well as present in the cytoplasm, in contact with different organelles.

The use of nanoparticle drug delivery technologies may improve chemotherapeutics distribution along with the reduction of the dose. Different preclinical investigations have focused in two classes of chemotherapeutics, including doxorubicin, paclitaxel, daunorubicin, and docetaxel (Zhang et al. 2008).

Delivery of therapeutic genes has been studied and tested based on viral vectors and constitute a substantial hope to treat cancer, muscular dystrophy, and other genetic-based diseases. However, the use of viruses is a drawback that includes several biosecurity issues. In this way, the use of nonviral gene therapy-based either in antisense or plasmid DNA use is a groundbreaking application of nanotechnology. In this scenario, CNTs have demonstrated remarkable capability in delivery of both DNA and siRNA. Traditional nonviral gene deliver (e.g., Lipofectamine)

substances present variable cytotoxicity, which is attributed to the destabilization of the cell membrane. Interestingly, Pantarotto et al. (2004b) observed that DNA carbon nanotube complexes do not increase cell proliferation or develop any toxic effects on cultured lymphocytes.

More recently, it has been shown that nanotubes may spontaneously insert the hydrophilic functional groups into a lipid bilayer so that they may enter cells without any membrane alterations or dysfunctions (Kam et al. 2004). Wang et al. (2008) have demonstrated that targeted RNA interference of cyclin A reduces the proliferation of K562 cells. The siRNA interference was carried out with SWCNTs and indicated a possibly useful therapeutic option for chronic myelogenous leukemia.

Overall, data indicates that the use of nanotechnology, especially the application of carbon nanotubes will contribute to new treatments that will be more efficient and targeted to cancer cells. In this way, therapies will be more efficient and result in less adverse side effects of chemotherapeutic drugs.

2.3.2 Cell Growth and Stem Cell Therapy

Cell culture is mostly based on substrate attachment that is achieved by electric charged surfaces and coating with different molecules. Cell adhesion is an important prerequisite for culture viability, protein expression, and multiplication. Also, certain cell types, such as neurons, are highly dependant on well-defined substrate so that axonal growth and synaptic formation is a function of an adequate growth permissive environment.

The use of CNTs may enhance cell adhesion, differentiation, migration, multiplication, and survival. In this sense, Mattson et al. (2000) have shown that MWCNTs support cultured primary hippocampal neurons and provide permissive substrate for axonal and neurite development and growth. The authors have shown that axons extended across the nanotubes coating, reaching the polyethyleneimine-treated glass surface. For this experiment, 20 nm diameter and 20–100 μm long particles were used and neurons attached to the nanotubes extended up to two neurites that grew to a distance range of 70–90 μm in 3 days. Interestingly, neurons survived and kept viable at least up to 8 days in vitro.

As mentioned before, carbon nanotubes have the remarkable feature of functionalization, by different chemical approaches. Modifications in the CNT structure, by the physical association of 4-hydroxynonenal (4-HNE), led to a remarkable increase in the number of neurites formed by hippocampal neurons, increasing from 1–2 to 4–6 projections. Also, much more elaborated networks were formed. In total, a threefold increase in the number of neuronal branches could be observed (Mattson et al. 2000).

In another work, Zhang et al. (2009) have associated different polysaccharides to single-walled carbon nanotubes in order to produce nanofibrous scaffolds. The results demonstrated that surface properties, regarded as a result of CNT coating,

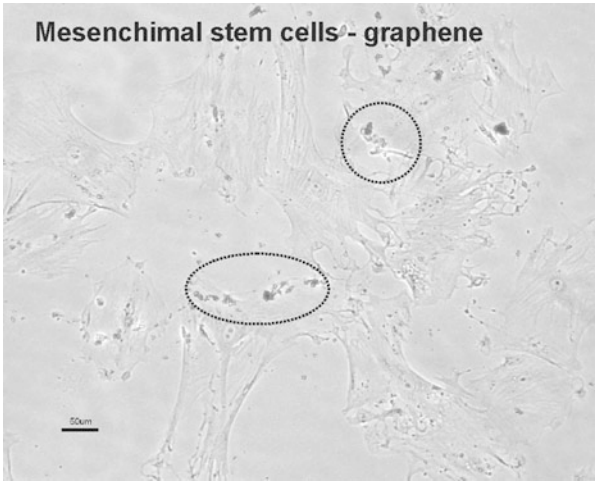


Fig. 2.7 Mesenchymal stem cells cultured in the presence of graphene (1 mg/mL). Observe the accumulation of nanoparticles inside the cells, which appear morphologically normal (picture from Prof. Dr. Alexandre L. R. Oliveira personal archive)

enhanced HeLa cells adhesion and proliferation. In our lab, we have also observed the beneficial effects of graphene and nanotubes of carbon on mesenchymal stem cells. As seen in Fig. 2.7, CNTs enter and accumulate inside the cultured cells without affecting cell proliferation and stability.

Additionally to the intrinsic properties of CNTs, the possibility of generating 2D and 3D organized substrates may further increase their usability in tissue regeneration. In this way, Zang and Yang (2011) have proposed a 3D scaffold produced with multiwalled carbon nanotube-coated polyethylene terephthalate (PET). The substrate was tested for cultivation of mouse embryonic stem cells and provided excellent cell viability and growth. It is possible that similar platforms may in turn facilitate stem cells culture and differentiation, providing new technologies for tissue engineering.

2.3.3 Peripheral Nerve Regeneration

The central nervous system, when compared to the peripheral counterpart, presents a higher regenerative capacity, although a complete recovery is rare (Ide 1996; Pereira Lopes et al. 2006).

The success of the peripheral nerve regeneration depends on the severity of the lesion. Seddon (1943) divided the nerve injuries in three categories according to the seriousness of the lesion: (1) Neuropraxia, which is the milder, when the axons are not ruptured and the continuity of the nerve is preserved. In this case, only a transitory loss of function is observed. (2) Axonotmesis, when the axons are sectioned but the epi-, peri-, and endoneurium are preserved. In this case, loss of function is more persistent, and depending on the proximity to the CNS, several months are necessary for complete recovery. (3) Neurotmesis, which represents the

complete transection of the nerve, generating two stumps. The proximal stump is connected to the neuron cell body and the distal stump that remains disconnected from the CNS. This lesion requires surgical repair and the outcome is variable, usually resulting in sensory and motor sequels.

Lesions that produce a loss of continuity of the nerve can be restored by suturing the stumps, what is called neurorrhaphy (Guénard et al. 1992; Grecco et al. 2003). Fibrin glue can also be used to reconnect the stumps (Martins et al. 2005; Sandrini et al. 2007). However, in many instances, the distance between the stumps is too large and the use of nerve grafts is necessary (Moroder et al. 2011). Nevertheless, autografting results in loss of function at the donor nerve site, and usually such nerves are too thin to repair the lesioned nerves (Evans 2000; Nakamura et al. 2004; Pierucci et al. 2008; Bockelmann et al. 2011; Moroder et al. 2011). As an alternative, tubular prostheses have been proposed to overcome longer gaps (Cunha et al. 2011). Such tubes may be resorbable, permeable to cells and molecules, and may be associated with nanoparticles, in order to enhance the nerve regeneration process (Pereira Lopes et al. 2006). The tubulization technique offers orientation and protection to the regenerating axons and has advantages over autografting, including the preservation of the donor nerve area and the potential to modify the microenvironment inside the prosthesis in order to improve the regenerative process (Dubey et al. 1999; Torres et al. 2003).

The main materials used to construct tubular prostheses are poly(α-hydroxy acids), which are considered as the most promising group of bioresorbable polymers (Baraúna et al. 2007). They include the poly(glycolic acid) (PGA), poly (dioxanone) (PDD), poly(L-lactic acid) (PLLA), and the poly(ε-caprolactone) (PCL) (Rezwan et al. 2006; Sun et al. 2010).

Nanoscaled scaffolds have also been used to enhance neuronal growth (Maturana et al. 2011). Results from our laboratory indicate an improved axonal growth and accumulation of nanoparticles in the ECM compartment, as seen in Fig. 2.8.

The nanostructures of carbon are indeed one of the most promising for enhancing neuronal regeneration and include CNTs, graphene sheets, and carbon nanofibers (Armentano et al. 2010). In this sense, Liao et al. (2012) observed that PLLA/PCL membranes, when associated with CNTs, presented enhancement of the mechanical properties, which led to a better biodegradation, cell proliferation, and orientation. Graphene nanocomposites may also improve the resistance to traction as well as to improve the electric conductivity and the thermic stability (Zhu et al. 2010). These are particularly important for biomedical applications, especially for neuronal growth and regeneration, since neurons actively generate and transport action potentials (Kotov et al. 2009). Li et al. (2011) described that films of graphene present excellent biocompatibility for hippocampal primary neuron cultures, leading to the formation of dendrites and axons, especially during the early development stages.

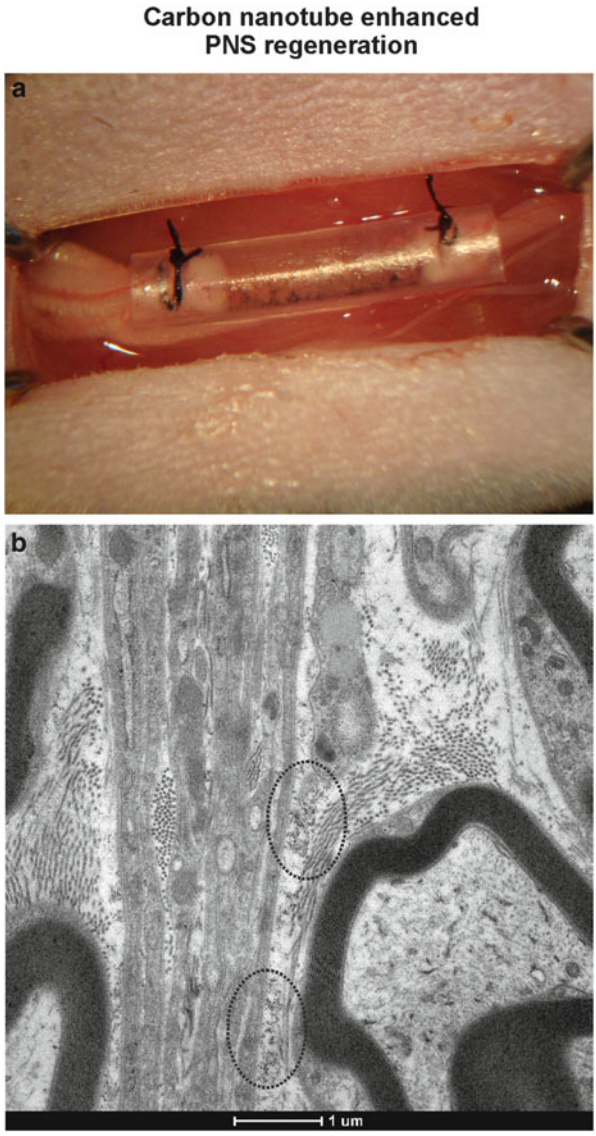


Fig. 2.8 (**a**) Tubulization of the sciatic nerve using polyethylene prosthesis. The gap between the stumps was filled with a saline solution containing CNTs. (**b**) CNT accumulation in between regenerated axons, 6 weeks following sciatic nerve tubulization (pictures from Prof. Dr. Alexandre L. R. Oliveira personal archive)

2.3.4 Biosensor

Modified carbon nanotubes and more recently graphene may be used as biosensors due to their unique electronic structure that can allow electrical detection of binding events. Several groups have proposed the use of SWNTs as consistent biosensors. One example is the work by Chen et al. (2012) that investigated carbohydrate-lectin interactions with both SWCNTs and chemically converted graphene. Such

nanostructures were obtained in order to develop nanoscaled biosensors to detect several bacteria-derived lectins, what may in turn allow rapid identification of such microorganisms in water systems, soil, and human samples, helping the public health system.

DNA detectors were also proposed by Star et al. (2006). The authors have created nanotube network field-effect transistors that selectively detect tagged DNA sequences. Such approach may help to develop highly effective, low cost, and low complexity systems for molecular diagnostics.

Interestingly, even the enzymatic degradation of starch can be monitored electronically using single-walled carbon nanotubes as semiconductor probes (Star et al. 2004).

More recently, Valentini et al. (2013) have proposed the assembly of amperometric biosensors modified by the use of carbon nanomaterial–hemin nanocomposite for direct electrochemical detection of environmental pollutants, for example, nitrite and H_2O_2.

Overall, it is clear that nanobiotechnology is a fast-growing field that will improve the quality and efficiency of numerous devices, particularly those destinated for the treatment of human diseases and lesions.

Acknowledgement Support from FAPESP, CNPq, and Brazilian Network on Nanotoxicology (MCTI/CNPq) and NanoBioss (MCTI) are acknowledged.

References

Armentano I, Dottori M, Fortunati E et al (2010) Biodegradable polymer matrix nanocomposites for tissue engineering: a review. Polym Degrad Stab 95:2126–2146

Balasubramanian K, Burghard M (2005) Chemically functionalized carbon nanotubes. Small 1:180–192

Baraúna GS, Pierucci A, Oliveira ARL et al (2007) Estudo da degradação "in vivo" de poli (L-co-D, L-ácido láctico) aplicado como prótese para regeneração nervosa periférica. Rev Matéria 12:298–306

Binnig G, Quate CF, Gerber C (1986) Atomic force microscope. Phys Rev Lett 56:930–933

Bockelmann J, Klinkhammer K, Holst A et al (2011) Functionalization of electrospun poly (ε-caprolactone) fibers with the extracellular matrix-derived peptide GRGDS improves guidance of Schwann cell migration and axonal growth. Tissue Eng 17:475–486

Bowie BT, Chase DB, Lewis IR et al (2002) Anomalies and artifacts in Raman spectroscopy. In: Chalmers JC, Griffiths PR (eds) Handbook of vibrational spectroscopy, vol 3. Wiley, Chichester

Bunaciu AA, Aboul-Enein HY, Fleschin S (2010) Application of Fourier transform infrared spectrophotometry in pharmaceutical drugs analysis. Appl Spectrosc Rev 45:206–219

Chan KLA, Kazarian SG, Vassou D et al (2006) In situ highthroughput study of drug polymorphism under controlled temperature and humidity using FT-IR spectroscopic imaging. Vib Spectrosc 43:221–226

Chen J, Hamon MA, Hu H (1988) Solution properties of single-walled carbon nanotubes. Science 282:95–98

Chen J, Rao AM, Lyuksyutov S et al (2001) Dissolution of full-length single-walled carbon nanotubes. J Phys Chem 105:2525–2528

Chen Y, Vedala H, Kotchey GP et al (2012) Electronic detection of lectins using carbohydrate functionalized nanostructures: Graphene versus carbon nanotubes. ACS Nano 6:760–770
Cunha C, Panseri S, Antonini S (2011) Emerging nanotechnology approaches in tissue engineering for peripheral nerve regeneration. Nanomedicine 7:50–59
Das RS, Agrawal YK (2011) Raman spectroscopy: recent advancements, techniques and applications. Vib Spectrosc 57:163–176
Dubey N, Letourneau PC, Tranquillo RT (1999) Guided neurite elongation and Schwann cell invasion into magnetically aligned collagen in simulated peripheral nerve regeneration. Exp Neurol 158:338–350
Esumi K, Ishigami M, Nakajima A et al (1996) Chemical treatment of carbon nanotubes. Carbon 34:279–281
Evans GRD (2000) Challenges to nerve regeneration. Semin Surg Oncol 19:312–318
Fernando KAS, Lin Y, Sun YP (2004) High aqueous solubility of functionalized single-walled carbon nanotubes. Langmuir 20:4777–4778
Georgakilas V, Otyepka M, Bourlinos AB et al (2012) Functionalization of graphene: covalent and non-covalent approaches, derivatives and applications. Chem Rev 112:6156–6214
Grecco MAS, Leite VM, Albertoni WM et al (2003) Estudo da regeneração nervosa em nervos tibiais de ratos Wistar utilizando o Fluoro-Gold® como marcador neuronal. Acta Ortop Bras 11:225–229
Guénard V, Kleitman N, Morrisey TK et al (1992) Syngeneic Schwann cells derived from adult nerves seeded in semipermeable guidance channels enhance peripheral nerve regeneration. J Neurosci 12:3310–3320
Guimarães AE, Pacheco MTT, Silveira L Jr et al (2006) Near infrared Raman spectroscopy (NIRS): a technique for doping control. Spectroscopy 20:185–194
Haguenau F, Hawkes PW, Hutchison JL et al (2003) Key events in the history of electron microscopy. Microsc Microanal 9:96–138
Hamon MA, Chen J, Hu H et al (1999) Dissolution of single-walled carbon nanotubes. Adv Mater 11:834–840
Hamon MA, Hui H, Bhowmik P et al (2002) Ester-functionalized soluble single-walled carbon nanotubes. Appl Phys A 74:333–338
Hanlon EB, Manoharan R, Koo T-W et al (2000) Prospects for in vivo Raman spectroscopy. Phys Med Biol 45:R1–59
Hirsch A (2002) Functionalization of single-walled carbon nanotubes. Angew Chem Int Ed 41:1853–1859
Hirsch A, Vostrowsky O (2005) Functionalization of carbon nanotubes. Top Curr Chem 245:193–237
Ide C (1996) Peripheral nerve regeneration. Neurosci Res 25:101–121
Inahara J, Touhara H, Mizuno T et al (2002) Fluorination of cup-stacked carbon nanotubes, structure and properties. Fluorine Chem 114:181–188
Jeon Y, Chang DW, Kumar NA et al (2011) Functionalization of carbon nanotubes. In: Yellampalli S (ed) Carbon nanotubes—polymer nanocomposites, InTech. http://www.intechopen.com/books/carbon-nanotubes-polymernanocomposites/functionalization-of-carbon-nanotubes
Kam NWS, Jessop TC, Wender PA et al (2004) Nanotube molecular transporters: internalization of carbon nanotube-protein conjugates into Mammalian cells. J Am Chem Soc 126:6850
Katz E, Willner I (2004) Biomolecule-functionalized carbon nanotubes: applications in nanobioelectronics. Chem Phys Chem 5:1085–1104
Kelly KF, Chiang IW, Mickelson ET et al (1999) Insight into the mechanism of sidewall functionalization of single-walled nanotubes: an STM study. Chem Phys Lett 313:445–450
Kotov NA, Winter JO, Clements IP et al (2009) Nanomaterials for neural interfaces. Adv Mater 21:3970–4004

Krafft C, Shapoval L, Sobottka SB et al (2006) Identification of primary tumors of brain metastases by SIMCA classification of IR spectroscopic images. Biochim Biophys Acta Biomembr 1758:883–891

Li N, Zhang X, Song Q et al (2011) The promotion of neurite sprouting and outgrowth of mouse hippocampal cells in culture by graphene substrates. Biomaterials 32:9374–9382

Liao G-Y, Zhou X-P, Chen L et al (2012) Electrospun aligned PLLA/PCL/functionalised multiwalled carbon nanotube composite fibrous membranes and their bio/mechanical properties. Compos Sci Technol 72:248–255

Liu J, Rinzler AG, Dai H et al (1998) Fullerene pipes. Science 280:1253–1256

Marcoux PR, Hapiot P, Batail P et al (2004) Electrochemical functionalization of nanotube films: growth of aryl chains on single-walled carbon nanotubes. New J Chem 28:302–307

Martel R, Shea HR, Avouris P (1999) Rings of single-walled carbon nanotubes. Nature 398:299

Martins RS, Siqueira MG, Silva CF, Plese JPP (2005) Overall assessment of regeneration in peripheral nerve lesion repair using fibrin glue, suture, or a combination of the 2 techniques in a rat model. Which is the ideal choice? Surg Neurol 64:10–16

Mattson MP, Haddon RC, Rao AM (2000) Molecular functionalization of carbon nanotubes and use as substrates for neuronal growth. J Mol Neurosci 14:175–182

Maturana LG, Zanon RG, Pierucci A, et al (2011) Supraorganized collagen enhances Schwann cell reactivity and organization in vitro. Braz J Med Biol Res 44:682–687.

Moreira LM, Silveira L Jr, Santos FV et al (2008) Raman spectroscopy: a powerful technique for biochemical analysis and diagnosis. Spectroscopy 22:1–19

Moroder P, Runge MB, Wang H et al (2011) Material properties and electrical stimulation regimens of polycaprolactone fumarate–polypyrrole scaffolds as potential conductive nerve conduits. Acta Biomater 7:944–953

Movasaghi Z, Rehman S, Rehman I (2008) Fourier transform infrared (FTIR) spectroscopy of biological tissues. Appl Spectrosc Rev 43:134–179

Nakamura T, Inada Y, Fukuda S et al (2004) Experimental study on the regeneration of peripheral nerve gaps through a polyglycolic acid–collagen (PGA–collagen) tube. Brain Res 1027:18–29

Niyogi S, Bekyarova E, Itkis ME et al (2010) Spectroscopy of covalently functionalized graphene. Nano Lett 10:4061–4066

Pantarotto D, Briand J-P, Prato M, Bianco A (2004a) Translocation of bioactive peptides across cell membranes by carbon nanotubes. Chem Commun 1:16–17

Pantarotto D, Singh R, McCarthy D et al (2004b) Functionalized carbon nanotubes for plasmid DNA gene delivery. Angew Chem Int Ed 43:5242–5246

Parker SF (1994) A review of the theory of Fourier-transform Raman spectroscopy. Spectrochim Acta 50A:1841–1856

Pawley J (1997) The development of field-emission scanning electron microscopy for imaging biological surfaces. Scanning 19:324–336

Pereira Lopes FR, Campos LCM, Corrêa JD Jr et al (2006) Bone marrow stromal cells and resorbable collagen guidance tubes enhance sciatic nerve regeneration in mice. Exp Neurol 198:457–468

Pereira RS (2001) Atomic force microscopy as a novel pharmacological tool. Biochem Pharmacol 62:975–983

Pierucci A, Duek EAR, Oliveira ALR (2008) Peripheral nerve regeneration through biodegradable conduits prepared using solvent evaporation. Tissue Eng 14:595–606

Prato M, Kostarelos K, Bianco A (2008) Functionalized carbon nanotubes in drug design and discovery. Acc Chem Res 41:60–68

Rattanaa T, Chaiyakun S, Witit-anun N et al (2012) Preparation and characterization of graphene oxide nanosheets. Procedia Eng 32:759–764

Rezwan K, Chen QZ, Blaker JJ et al (2006) Biodegradable and bioactive porous polymer/inorganic composite scaffolds for bone tissue engineering. Biomaterials 27:3413–3431

Sandrini FAL, Pereira-Júnior ED, Gay-Escoda C (2007) Anastomose do nervo facial de coelhos com cola de fibrina: estudo da velocidade de condução nervosa. Rev Bras Otorrinolaringol 73:196–201

Seddon HJ (1943) Three types of nerve injury. Brain 66:237–288

Stadtländer CTK-H (2007) Scanning electron microscopy and transmission electron microscopy of mollicutes: challenges and opportunities. In: Méndez-Vilas A, Díaz J (eds) Modern research and educational topics in microscopy. Formatex, Badajoz

Star A, Joshi V, Han TR et al (2004) Electronic detection of the enzymatic degradation of starch. Org Lett 24:2089–2092

Star A, Tu E, Niemann J et al (2006) Label-free detection of DNA hybridization using carbon nanotube network field-effect transistors. PNAS 103:921–926

Sun M, Kingham PJ, Reid AJ et al (2010) In vitro and in vivo testing of novel ultrathin PCL and PCL/PLA blend films as peripheral nerve conduit. J Biomed Mater Res A 93(4):1470–1481

Tagmatarchis N, Prato M (2004) Functionalization of carbon nanotubes via 1,3-dipolar cycloadditions. J Mater Chem 14:437–439

Tasis D, Tagmatarchis N, Bianco A, Prato M (2006) Chemistry of carbon nanotubes. Chem Rev 106:1105–1136

Torres MFP, Graça DL, Farias ELP (2003) Reparação microcirúrgica de nervo periférico por meio de sutura, cola de fibrina ou bainha de BioFill® em ratos Wistar. Arq Bras Med Vet Zootec 5:557–561

Unger E, Graham A, Kreupl F et al (2002) Electrochemical functionalization of multi-walled carbon nanotubes for solvation and purification. Curr Appl Phys 2:107–111

Valentini F, Carbone M, Palleschi G (2013) Carbon nanostructured materials for applications in nano-medicine, cultural heritage, and electrochemical biosensors. Anal Bioanal Chem 405:451–465

Voutou B, Stefanaki E-C (2008) Electron microscopy: the basics. physics of advanced materials winter school. Aristotle University of Thessaloniki, Greece

Wang X, Ren J, Qu X (2008) Targeted RNA interference of cyclin A2 mediated by functionalized single-walled carbon nanotubes induces proliferation arrest and apoptosis in chronic myelogenous leukemia K562 cells. ChemMedChem 3:940–945

Wang Y, McCreery RL (1989) Evaluation of a diode laser/charge coupled device spectrometer for near-infrared Raman spectroscopy. Anal Chem 61:2647–2651

Wang ZL (2000) Transmission electron microscopy of shape-controlled nanocrystals and their assemblies. J Phys Chem B 104:1153–1175

Woolley AT, Cheung CL, Hafner JH et al (2000) Structural biology with carbon nanotube AFM probes. Chem Biol 7:R193–R204

Wu X, Sun Z, Meininger GA, Muthuchamy M (2012) Application of atomic force microscopy measurements on cardiovascular cells. Methods Mol Biol 843:229–243

Yao H, Kimura K (2007) Field emission scanning electron microscopy for structural characterization of 3D gold nanoparticle superlattices. In: Méndez-Vilas A, Díaz J (eds) Modern research and educational topics in microscopy. Formatex, Badajoz

Zang X, Yang S-T (2011) High-throughput 3-D cell-based proliferation and cytotoxicity assays for drug screening and bioprocess development. J Biotechnol 151:186–193

Zhang J, Zou H, Qing Q et al (2003) Effect of chemical oxidation on the structure of single-walled carbon nanotubes. J Phys Chem B 107:3712–3718

Zhang L, Gu FX, Chan JM et al (2008) Nanoparticles in medicine: therapeutic applications and developments. Clin Pharmacol Ther 83:761–769

Zhang X, Meng L, Lu Q (2009) Cell behaviors on polysaccharide-wrapped single-wall carbon nanotubes: a quantitative study of the surface properties of biomimetic nanofibrous scaffolds. ACS Nano 3:3200–3206

Zhu Y, Murali S, Cai W et al (2010) Graphene and graphene oxide: synthesis, properties, and applications. Adv Mater 22:3906–3924



http://www.springer.com/978-1-4614-8992-4

Nanotoxicology
Materials, Methodologies, and Assessments
Durán, N.; Guterres, S.S.; Alves, O.L. (Eds.)
2014, XV, 411 p. 42 illus., 22 illus. in color., Hardcover
ISBN: 978-1-4614-8992-4